EHT Environmental Health and Toxicology

Open Access

Volume: 32, Article ID: e2017016, 8 pages
https://doi.org/10.5620/eht.e2017016

• Original Article

eISSN: 2233-6567

Morphological transformation induced by silver nanoparticles in a Balb/c 3T3 A31-1-1 mouse cell model to evaluate *in vitro* carcinogenic potential

Wunhak Choo, Byeonghak Moon, Sulhwa Song, Seung Min Oh

Department of Nanofusion Technology, Hoseo University, Asan, Korea

Carcinogenesis is a complex process involved in genotoxic and non-genotoxic pathways. The carcinogenic potential of silver nanoparticles (AgNPs) has been predicted by examining their genotoxic effects using several *in vitro* and *in vivo* models. However, there is no little information regarding the non-genotoxic effects of AgNPs related to carcinogenesis. The *in vitro* cell transformation assay (CTA) provides specific and sensitive evidence for predicting the tumorigenic potential of a chemical, which cannot be obtained by genotoxicity testing. Therefore, we carried out CTA in Balb/c 3T3 A31-1-1 cells to evaluate the carcinogenic potential of AgNPs. Colony-forming efficiency and crystal violet assays were carried out to determine the cytotoxicity of AgNPs. A cytokinesis-block micronucleus (CBMN) assay and CTA were performed using Balb/c 3T3 A31-1-1 cells to predict the *in vitro* carcinogenic potential of AgNPs. In the CBMN assay, AgNPs (10.6 μg/mL) induced a significant increase in micronucleus formation indicating a genotoxic effect. Thus, AgNPs could be an initiator of carcinogenesis. In the CTA, used to assess the carcinogenic potential of AgNPs, cells exposed to AgNPs for 72 hours showed significantly induced morphological neoplastic transformation at all tested doses (0.17, 0.66, 2.65, 5.30, and 10.60 μg/mL), and the transformation frequency was significantly increased in a dose-dependent manner. These results indicate that short-term exposure (72 hours) to AgNPs had *in vitro* carcinogenetic potency in Balb/c 3T3 A31-1-1 cells.

Keywords Silver nanoparticles, Cell transformation assay, *In vitro* carcinogenic potential, Balb/c 3T3 A31-1-1 cells

Correspondence: Seung Min Oh
Department of Nanofusion Technology, Hoseo University, 20 Hoseo-ro 79beon-gil, Asan 31499, Korea
E-mail: ohsmo403@hoseo.edu

Received: August 17, 2017
Accepted: October 7, 2017
Published: October 7, 2017

This article is available from: http://e-eht.org/

INTRODUCTION

The unique physicochemical properties of nanoparticles have led to their development for biomedical and industrial applications. Among the various nanoparticles, silver nanoparticles (AgNPs) are widely used in industrial and consumer products such as antimicrobial applications, biosensors, composite fibers, cryogenic superconducting materials, cosmetic products, and electronic components [1]. However, the widespread application of AgNPs has led to growing concerns about their potential adverse effects.

In the Integrated Risk Information System (http://www.epa.gov/iris/subst/0099.htm), the carcinogenic potential of silver (Ag) has been reported as Group D (not classified for human carcinogenicity) according to the results of limited animal studies, in which chronic subcutaneous administration of colloidal Ag into rats resulted in an increase in the incidence of malignant tumors [2], but the intramuscular injection of Ag (< 300 mesh) into rats was not reported to induce cancer [3]. In the nanotechnology field, nanoscale Ag particles with a diameter ranging from 1 to 100 nm have numerous commercial applications. Nanoparticles could have physicochemical characteristics different from those of larger size particle and could induce high reactivity due to their higher surface area [4]. Therefore, it is

possible to induce different results with AgNPs in terms of carcinogenicity, as reported in previous studies [2,3].

Carcinogenesis is induced by a multistep pathway, beginning with initiation, promotion, and finally progression [5,6]. Initiation, the first step in carcinogenesis, involves sequential genetic changes induced by DNA damage in a single target cell. Promotion and progression occur via non-genotoxic mechanisms that cause growth alterations and culminate in cells that are able to form malignant tumors [7].

The carcinogenic potential of AgNPs has been predicted by evaluating genotoxic effects using *in vitro* and *in vivo* models. AgNPs have been reported to significantly increase micronuclei formation in CHO-K1 cells [8], Syrian hamster embryo (SHE) cells [9], and HepG2 cells [10]. In addition, DNA damage caused by AgNPs has been reported in human microvascular endothelial cells [11] and A549 cells [12], assessed using the comet assay. Jiang et al. [8] reported that DNA adduct and 8-oxo-deoxyguanosine were induced by AgNPs. In animal studies of genotoxicity, albino rats administered repeated intraperitoneal injections containing AgNPs for 28 days showed hepatic histopathological alterations and chromosomal aberrations in bone marrow cells [13]. In addition, rats exposed only to AgNPs showed significantly enhanced micronuclei formation in polychromatic erythrocytes [14]. Li et al. [15] reported that AgNPs reach mouse bone marrow and liver where they have cytotoxic effects on reticulocytes and cause oxidative DNA damage in the liver. Based on these reports, AgNPs could be an initiator of the carcinogenesis processes.

In this study, we used a Balb/c 3T3 A31-1-1 mouse cell model, a major *in vitro* system for assessing carcinogenesis, to evaluate the carcinogenic potential of AgNPs. Firstly, the Ag nanopowder (< 100 nm), which was completely dispersed in an experimental medium by sonication, was characterized by energy dispersion X-ray spectrum (EDS) analysis, transmission electron microscopy (TEM), scanning electron microscopy (SEM), dynamic light scattering (DLS), and zeta potential. Secondly, colony-forming efficiency (CFE) and crystal violet (CV) assays were carried out to determine the cytotoxicity of AgNPs. Finally, a cytokinesis-block micronucleus (CBMN) assay and cell transformation assay (CTA) were performed in Balb/c 3T3 A31-1-1 cells to predict the *in vitro* carcinogenic potential of AgNPs.

METHODS

Materials

Benzo(a)pyrene (B[a]P; CAT No. B1760), anthracene (An; CAT No. A89200), and AgNPs (CAT No. 576832) were purchased from Sigma-Aldrich (St. Louis, MO, USA). Prior to treatment, chemicals (B[a]P and An) were dissolved in dimethyl sulfoxide (DMSO) and stored at -20°C until needed. The final concentration of the vehicle (DMSO) in the assay was adjusted to 0.5% (v/v).

Silver Nanoparticle Sample Preparation and Characterization

Ag nanoparticles (CAT No. 576832; Sigma-Aldrich) were homogeneously dispersed in minimum essential media (MEM) media (Gibco Invitrogen, Grand Island, NY, USA) by sonication for 30 minutes (Bioruptor UCD-200T; Cosmo Bio, Tokyo, Japan), then filtered through a cellulose membrane (0.45-μm pore size; Advantec, Tokyo, Japan). The concentration of filtered AgNPs measured by inductively coupled plasma (Optima 7300 DV; Perkin Elmer, Waltham, MA, USA) was 10.60 ± 0.44 μg/mL. The purity of AgNPs was assessed by EDS analysis (EMAX; Horiba, Kyoto, Japan). TEM (JEM 2100F; JEOL, Peabody, MA, USA) and SEM (Hitachi, Tokyo, Japan) were used to evaluate the size and shape of AgNPs. The size distribution of AgNPs dispersed in culture medium at the highest concentration (10.60 μg/mL) was measured by a DLS technique Sympatec GmbH Nanophox particle size analyzer (Clausthal-Zellerfeld, Germany), and the zeta potential was measured using ELS-Z (Otsuka Electronics Inc., Osaka, Japan).

Cell Culture Conditions

Balb/c 3T3 A31-1-1 cells were purchased from the Japanese Collection of Research Bioresources Cell Bank (Osaka, Japan). The cell line (mouse fibroblast cells) were grown in MEM supplemented with 10% fetal bovine serum (FBS; Hyclone, Logan, UT, USA), penicillin (100 U/mL), and streptomycin (100 μg/mL), and were maintained in a humidified incubator at 37°C in a 5% carbon dioxide/95% air atmosphere.

Cytokinesis-block Micronucleus Assay

The CBMN assay was performed to evaluate the genotoxic effects of AgNPs. The Balb/c 3T3 A31-1-1 cells were seeded onto 8-well chamber slides (4×10^4 cells/well) and cultured for 24 hours. The cells were treated with AgNPs at different concentrations (0.17, 0.66, 2.65, 5.30, and 10.60 μg/mL) in culture medium for 24 hours. The cells were washed two times with phosphate buffered saline (PBS) and treated with 1% trisodium citrate for 5 minutes at 4°C. The slides were then placed in fresh fixative (99:1 of methanol: acetic acid) at 4°C and left on a clean bench to air-dry before being placed in ribonuclease A (10 μg/mL in 2 × standard saline citrate (SSC) for 5 minutes at 30°C. The slide was then rinsed with 2 × SSC (0.02 M sodium citrate and 0.3 M sodium chloride) and left on a clean bench to air-dry.

After thorough air-drying, the slide was stained with 5% Giemsa solution for 20 minutes. According to the micronucleus (MN) scoring criterion, 500 binucleate cells per independent culture were obtained. To assess the toxicity to cells induced by cytochalasin-B, the cytokinesis-block proliferation index (CBPI) was measured as ([1×number of mononucleated cells]+[2×number of binucleated cells]+(3×number of trinucleated cells])/500 [16].

Range Finding for Crystal Violet Assay and Colony-forming Efficiency Assay

The Balb/c 3T3 A31-1-1 cells (passage 10) at approximately 80% confluency were trypsinized and suspended in M10F complete medium (10% FBS in MEM medium). Then, cells (passage 11) were seeded onto 6-well plates (3×10^3 cells/well/1.5 mL) or a 60 mm dish (200 cells/4 mL) containing M10F complete medium. After 24 hours incubation, the medium was changed to the treatment media (M10F) containing B(a)P (1 μg/mL) as a positive control, An (20 μg/mL) as the negative control, or AgNPs (0.17, 0.66, 2.65, 5.30, or 10.60 μg/mL). Cells exposed to the treatment medium for 3 days were washed two times with PBS, then the medium was replaced with fresh M10F complete medium. After another 3 days (CV) or 5 days (CFE), the cells were fixed and stained with 0.1% CV or 0.04% Giemsa solution to assess cell viability by the CV and CFE assay, respectively. In the CV assay, the stained dye in each well was extracted with 1.5 mL of extraction solution (50:49:1 of ethanol:distilled water:1M hydrogen chloride) and the optical density of each well was measured at 540 nm. In the CFE assay, the stained colonies (>50 cells or >2 mm in diameter) were scored according to image and stereological analysis with an optical system attached to an upright microscope (CX31; Olympus, Tokyo, Japan) and a digital camera (IMTi-solution Inc., Burnaby, BC, Canada).

Cell Transformation Assay

Balb/c 3T3 A31-1-1 cells (passage 10) at approximately 80% confluency were trypsinized and suspended in M10F complete medium. Then, cells (passage 11) were seeded onto a 100-mm dish at a density of 2×10^4 cells/10 mL of M10F complete medium. After 24 hours incubation, the medium was changed to the treatment media (M10F) containing B(a)P, An, or AgNPs. Cells exposed to the treatment medium for 72 hours were washed two times with PBS, then the medium was replaced with 10 mL of fresh Dulbeco's modified Eagle's media (DMEM)/FI2 complete medium. Thereafter, DMEM/FI2 medium was replaced every 3 days for a total of 25 days. At day 25, the medium was changed, and cells remained in culture for another 2 days. At day 27, the cells were fixed with methanol for 10 minutes then stained with a 0.04% Giemsa solution for 30 minutes. For the analysis of the CTA, foci consisting of more than about 50 cells or that were more than about 2 mm in diameter were evaluated using a stereomicroscope. Only type III foci were recorded, which are characterized by the following morphological criteria [17]: deep basophilic staining of spindle-shaped cells which were morphologically different to the background monolayer cells, dense multilayering of cells (piling up), random orientation, and invasive growth of cells at the edge of foci (criss-cross pattern). The transformation results were expressed as the transformation frequency (Tf; five replicates per concentration, two experiments performed) using the following formula: Tf=([A/B×C×D]), where A is the total number of type III foci per treatment; B is CFE (%)/100; C is the plating efficiency (%)/100; D is the number of cells seeded×number of plates; plating efficiency (%) is the number of colonies formed in the control×100/200, and 200 is the total number of cells seeded into one CFE dish [18].

Statistical Methods

Each assay was performed at least in triplicate. SigmaPlot 12.0 (Jandel Scentific, San Rafael, CA, USA) and Excel 2010 (Microsoft, Redmond, WA, USA) software were used to analyze the data. The data are expressed as mean±standard deviation. Statistical analysis was carried out using PASW 18.0 (SPSS Inc., Chicago, IL, USA). Statistical differences between the groups were determined using one-way analysis of variance followed by *t*-test. Statistical significance was accepted at $p<0.01$ or $p<0.05$.

RESULTS

Characterization of Silver Nanoparticles

The physicochemical properties of AgNPs dispersed in M10F medium were characterized by EDS, SEM, TEM, DLS, and zeta potential. The EDS analysis to evaluate AgNP purity showed that there were no other impurities present (Figure 1A). In the TEM and SEM analyses (Figure 1B and 1C), AgNPs were observed as spherical aggregates approximately 1-80 nm in size. As shown in Figure 1D and 1E (green box), the cumulative particle size of AgNPs measured by DLS ranged from 1 to 200 nm, and 84% of AgNPs had a diameter of <100 nm, with an average diameter size for AgNPs dispersed in M10F medium of 80.0±6.0 nm. About 600 particles were counted by SEM (Figure 1D and 1E, light green box), and 73.5% of AgNPs was observed to have a diameter <100 nm. The zeta potential of the AgNPs was -21.03±2.46 mV in M10F medium (data not shown).

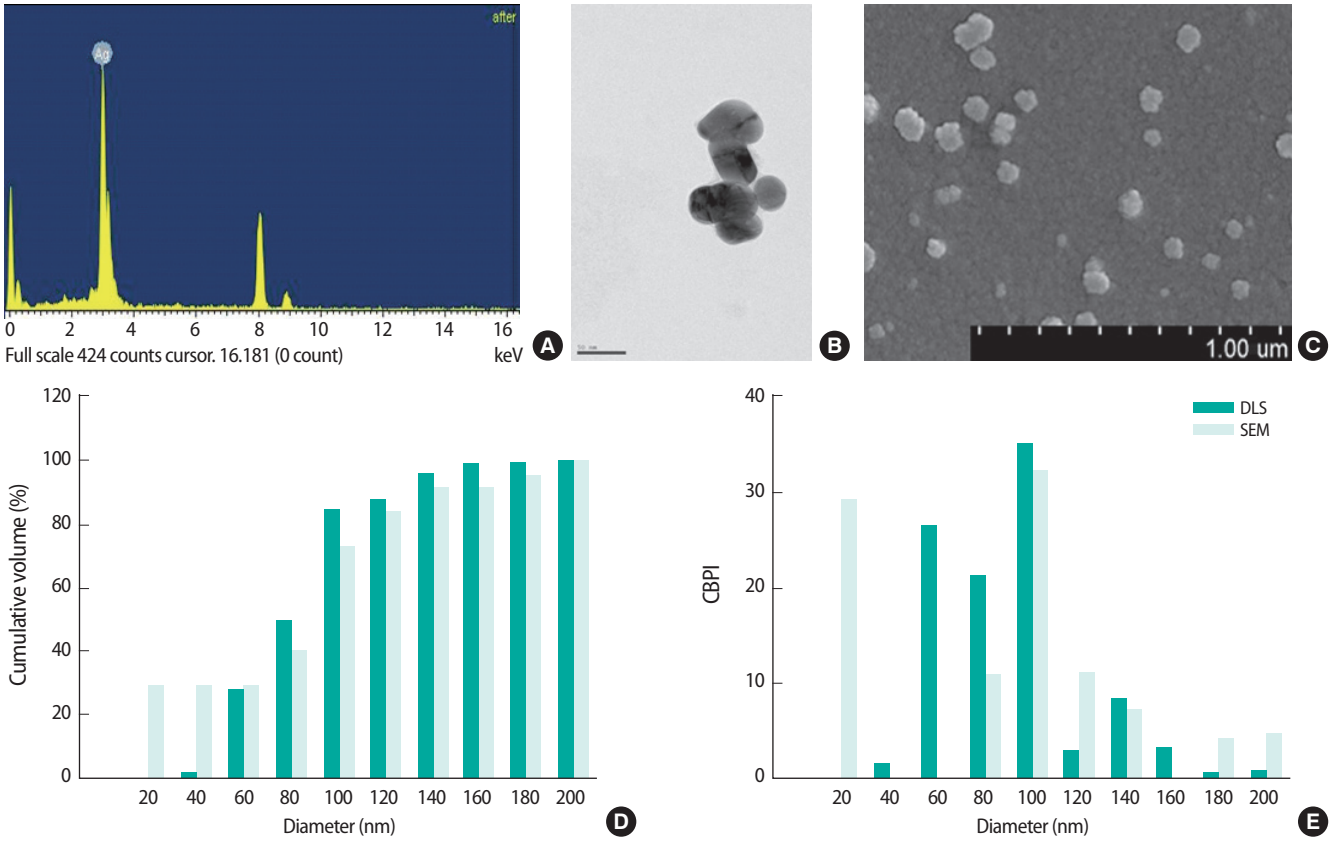

Figure 1. Characterization of silver nanoparticles (AgNPs) by (A) energy dispersion spectrum analysis, (B) transmission electron microscopy, and (C) SEM. The size distribution of AgNPs was measured by DLS and SEM counts (600 particles) of distribution, giving (D) the cumulative volume (%) and (E) size distribution (%). Cts, counts; CBPI, cytokinesis-block proliferation index; SEM, scanning electron microscopy; DLS, dynamic light scattering.

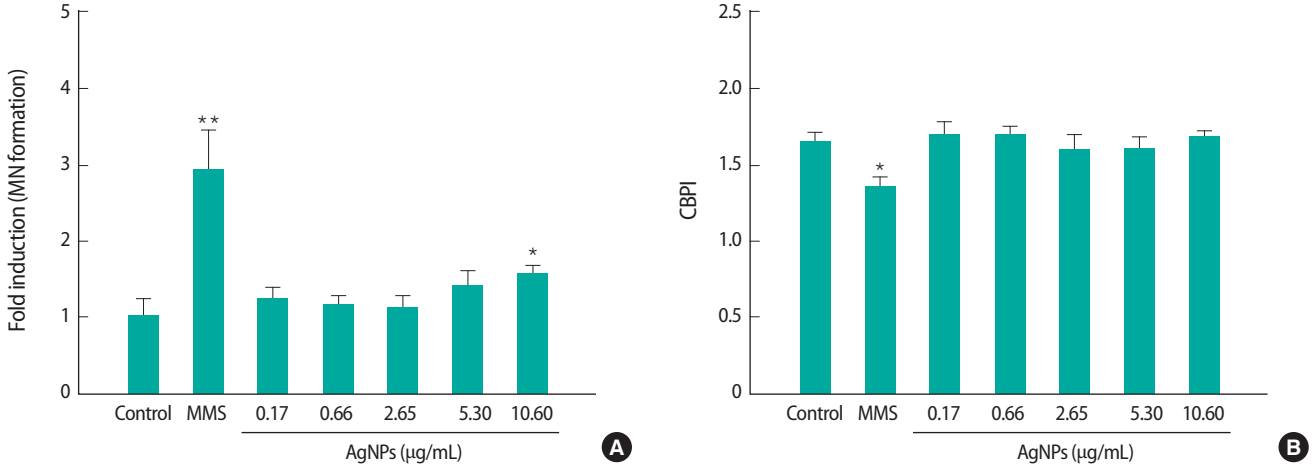

Figure 2. Micronucleus (MN) formation induced by silver nanoparticles (AgNPs) in Balb/c 3T3 A31-1-1 cells in the presence of cytochalasin B. (A) Micronucleus formation, (B) cytokinesis-block proliferation index (CBPI) index. Cells were treated with AgNPs (0.17, 0.66, 2.65, 5.30, or 10.60 μg/mL) or methyl methane sulfonate (MMS, 50 μg/mL) as the positive control. Results are expressed as the mean±standard deviation of three separate experiments for each data point for MN frequency per 500 binucleate cells. Values are significantly different from the control at *p<0.05 and **p<0.01.

Genotoxic Effects Assessed by Cytokinesis-block Micronucleus Assay

For the CBMN assay, Balb/c 3T3 A31-1-1 cells were exposed to AgNPs at 0.17, 0.66, 2.65, 5.30, or 10.60 μg/mL. These exposure concentrations did not show any cytotoxic effects in the sulforhodamine B and neutral red uptake assays (data not shown). MN formation was significantly increased in cells treated with the highest dose (10.60 μg/mL) of AgNPs, which was

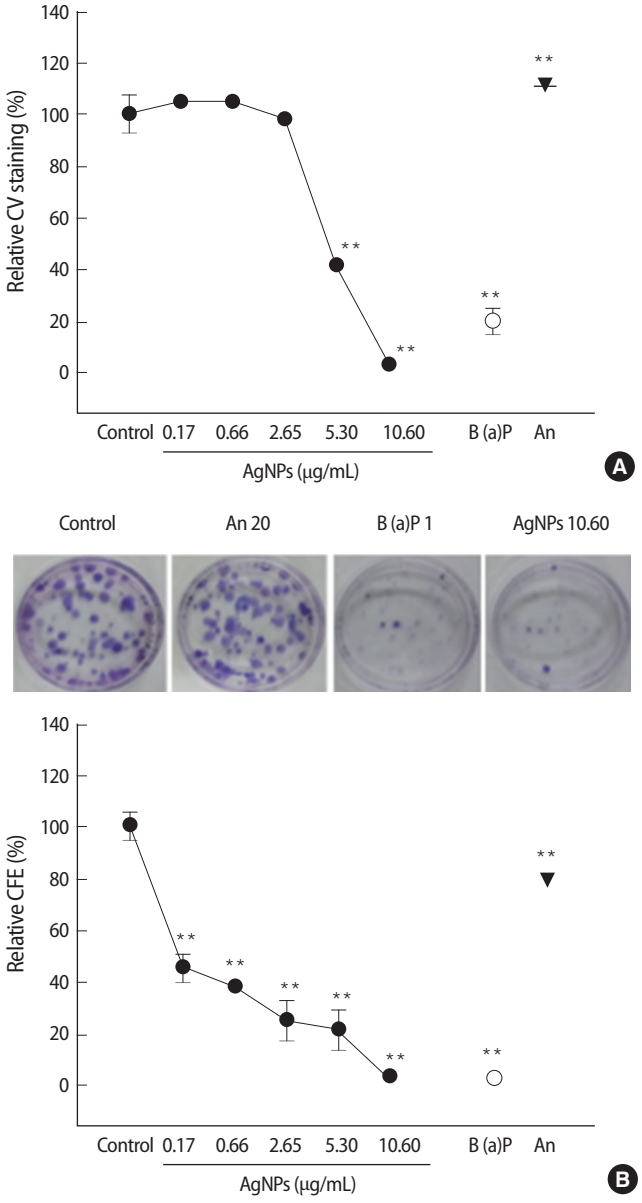

Figure 3. Cytotoxic effects of test compounds in the Balb/c 3T3 A31-1-1 cell line assessed by (A) crystal violet (CV) assay and (B) colony-formation assay (CFE). The cells were treated with silver nanoparticles (AgNPs), (0.17, 0.66, 2.65, 5.30, or 10.60 μg/mL), benzo(a)pyrene (B[a]P, 1 μg/mL), or anthracene (An, 20 μg/mL) for 72 hours. The cytotoxic effect of the compounds was presented relative to the control. Results are expressed as the mean±standard deviation of three separate experiments. **p<0.01.

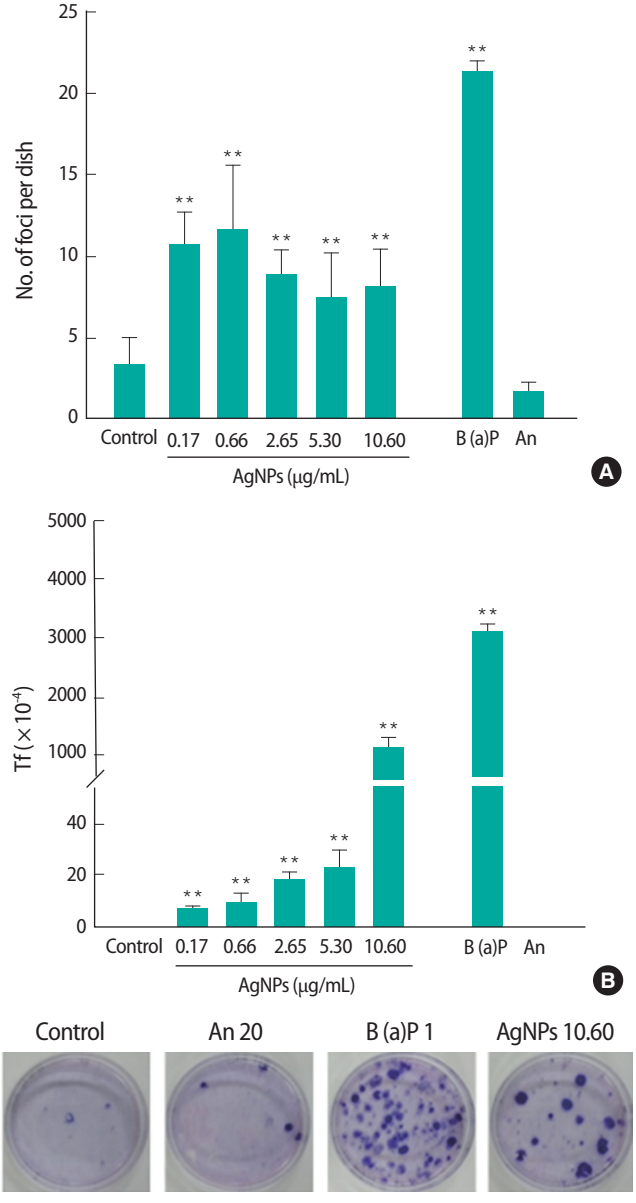

Figure 4. Morphological neoplastic transformation induced by silver nanoparticles (AgNPs) in Balb/c 3T3 A31-1-1 cells. (A) Number of foci per plate, (B) transformation results (Tf). Cells were seeded onto a 100-mm dish and treated with AgNPs (0.17, 0.66, 2.65, 5.30, or 10.60 μg/mL), benzo(a) pyrene (B[a]P, 1 μg/mL), or anthracene (An, 20 μg/mL). Transformation frequency (Tf) was calculated as indicated in the materials and methods section. Results are expressed as the mean±standard deviation. **p<0.01.

increased by about 1.6 times compared to the control. The CBPI was approximately 1.6 in all AgNP-treated groups, but there was no distinct difference between groups except for the positive control (methyl methane sulfonate, 50 μg/mL) (Figure 2).

Cytotoxicity Measured by Crystal Violet and Colony-forming Efficiency Assays

The cytotoxicity of the test compounds was investigated by CV and CFE assays. As assessed by the CV and CFE assay (Figure 3), cell viability was significantly decreased in Balb/c 3T3 A31-1-1 cells exposed to AgNPs in a dose-dependent manner. As shown in Table 1, the concentration resulting in 50% inhibition of cell viability (IC_{50}) and concentration resulting in 90% inhibition of cell viability (IC_{90}) of AgNPs were 5.91 and 9.59, respectively, in the CV assay, while the IC_{50} and IC_{90} of AgNPs were found to be 0.17 and 9.34, respectively, in the CFE assay.

Table 1. Cytotoxicity of AgNPs in the Balb/c 3T3 A31-1-1 cell line

AgNPs (μg/mL)	CV	CFE
NOAEC	2.65	-
IC_{50}	5.91	0.17
IC_{90}	9.59	9.34

AgNPs, silver nanoparticles; CV, crystal violet; CFE, colony-formation assay; NOAEC, no observed adverse effect concentration; IC_{50}, concentration resulting in 50% inhibition of cell viability; IC_{90}, concentration resulting in 90% inhibition of cell viability.

Morphological Transformation

As shown in Figure 4A, the morphological neoplastic transformation of AgNPs was investigated by CTA in Balb/c 3T3 A31-1-1 cells. The number of foci per plate was significantly increased in all groups exposed to AgNPs compared to the control group. In particular, cells exposed to 0.17 μg/mL AgNPs showed an approximate 3-fold increase in the formation of type III foci compared to the control group. The positive control (B[a]P) showed 21.33-fold increase of foci formation per plate, but the negative control (An) showed no increase in foci formation compared to the control. Figure 4B shows the transformation results (Tf) assessed by the CTA assay, calculated from the type III foci count and cytotoxicity index (CFE). The Tf of 1 μg/mL B(a)P and 10.60 μg/mL AgNPs were 3124.38 ± 198.59 and 1088.53 ± 198.59, respectively.

DISCUSSION

According to the European Commission [19], a nanomaterial (NM) must contain at least 50% small particles with a diameter between 1 and 100 nm, which may exist in an unbound state or in an aggregate or agglomerate state. The AgNPs used in our study contained 80% particles smaller than 100 nm in diameter (Figure 1), which means that the AgNPs is being maintained as a NM. The broad use of AgNPs as industrial, household, and healthcare-related products could lead to increased exposure in humans, therefore, further studies on their toxicological effects are required. In this study, we investigated the carcinogenic potential of AgNPs in Balb/3T3 A31-1-1 mouse fibroblasts by CBMN and morphological transformation assays.

Carcinogenesis is a complex process involving both genotoxic and non-genotoxic pathways. Initiation, the first step in carcinogenesis, is related to sequential genotoxic changes induced by DNA damage in a single target cell. Since 2012, genotoxicity studies on AgNPs have shown positive genotoxic effects in several *in vitro* [8-12] and *in vivo* [13-15] tests. In the current study, MN formation induced by AgNP exposure (10.60 μg/mL) for 24 hours was increased in the Balb/c 3T3 A31-1-1 mouse fibroblast cell line, as measured by the CBMN assay (Figure 2). The CBMN method has been widely used to evaluate genotoxic effects such as chromosome breakage, impaired DNA repair, chromosome loss, non-disjunction, necrosis, apoptosis, and cytostasis [20]. Similar to our results, exposure to AgNPs (0.01-10.00 μg/mL) for 24 hours has previously been reported to induce a significant increase in MN formation in BEAS-2B cells [21] and CHO-K1 cells [22], as detected by the CBMN assay. Li et al. [9] found significant MN formation using the CBMN assay in SHE cells exposed to 20 μg/mL AgNPs. In a flowcytometric-based MN assay, AgNPs exposure for 24 hours induced significant MN formation in HepG2 cells (5 μg/mL) [10], CHO-K1 cells (5 μg/mL) [8], and TK6 cells (25 μg/mL) [23]. The effective concentration (10.60 μg/mL) of AgNPs in our study is comparable to that published by others (0.01-20.00 μg/mL). In contrast, Broggi et al. [24] showed a negative impact of AgNPs on MN formation in the same cell line used in our study. In dispersion conditions without the use of a stabilizing agent, the diameter of AgNPs in our study was 80.0 ± 6.0 nm, which is smaller than that reported in the study by Broggi et al. [24] (117.8 ± 16.6 nm). In addition, the effective concentration (10.60 μg/mL) of AgNPs in our study was higher than the exposure concentration (0.11-1.08 μg/mL) of AgNPs reported by Broggi et al. [24]. Therefore, we suggest that the positive results obtained in our study may be due to differences in size and exposure concentration compared to the study by Broggi et al. [24]. Several *in vivo* MN tests of AgNPs have shown controversial results. In male and female Sprague-Dawley rats, inhalation exposure to AgNPs for 90 days did not have any genotoxic effects on bone marrow [21]. When AgNPs were intravenously injected [14], micronucleated reticulocytes were not observed, although MN formation in the liver was enhanced. In addition, Dobrzyńska et al. [14] reported that AgNPs induced MN formation in polychromatic erythrocytes, but not in reticulocytes and leukocytes. These results indicate that susceptibility to AgNP-induced genotoxicity differ between bone marrow cells and organs. The genotoxicity of AgNPs is a controversial issue, and a clear genotoxic effect of AgNPs has been confirmed in both *in vitro* and *in vivo* model systems by us and several other authors. Therefore, we suggest that the genotoxic potential of AgNPs indicates an important role as an initiator of carcinogenesis.

The *in vitro* CTA can provide specific and sensitive evidence for predicting the tumorigenic potential of a chemical which cannot be supplied by genotoxicity testing [25]. CTA has been considered an alternative *in vitro* method as it closely models the carcinogenic process of a rodent 2-year carcinogenesis bioassay [26-28]. Therefore, in this study, CTA in the Balb/3T3 A31-1-1 mouse fibroblast cell line was used to evaluate the carcinogenic potential of AgNPs. Firstly, the appropriate dose-range for the

transformation assay was based on the data (no observable adverse effective concentration, IC_{50} and IC_{90}) obtained by the CV and CFE assays [17]. In the current study, the IC_{50} (0.17 μg/mL) determined by the CFE assay was more sensitive than that determined by the CV assay (5.91 μg/mL), therefore, doses for the morphological transformation experiment were selected based on the results of the CV experiments (Figure 3). At the exposure dose (0.17-10.60 μg/mL), determined based on the CTA results, AgNPs induced a morphological neoplastic transformation (Figure 4). Choo et al. [29] previously reported that long-term exposure to a low-dose (0.13 and 1.33 μg/mL) of AgNPs enhanced *in vitro* malignant cell transformation in non-tumorigenic BEAS-2B cells. The results of Choo et al. [29] support our results. However, Broggi et al. [24] reported a negative result in regard to morphological neoplastic transformation induced by AgNP exposure (0.11-1.08 μg/mL). Like CBMN result, Broggi et al. [24] used different exposure doses and AgNP sizes than those used in our study. Until now, the carcinogenic potential of AgNPs was a controversial issue. Although the results obtained in the current study confirm the possible role of AgNPs as an initiator and promotor of the carcinogenesis process, these were limited to an *in vitro* system. Therefore, further animal studies are required to identify any potential carcinogenic effects of AgNPs.

ACKNOWLEDGEMENTS

This work was supported by a grant from the Korea Ministry of Environment through the Environmental Health R&D Program (2012 001370009) and the National Research Foundation of Korea funded by the Korean government (NRF-2013R1A1A2A10060109).

CONFLICT OF INTEREST

The authors have no conflicts of interest associated with the material presented in this paper.

ORCID

Wunhak Choo *https://orcid.org/0000-0002-8350-740X*
Byeonghak Moon *https://orcid.org/0000-0002-2018-6418*
Sulhwa Song *https://orcid.org/0000-0001-5216-6633*
Seung Min Oh *https://orcid.org/0000-0002-5701-8960*

REFERENCES

1. Ahamed M, Alsalhi MS, Siddiqui MK. Silver nanoparticle applications and human health. Clin Chim Acta 2010;411(23-24):1841-1848.
2. Schmaehl D, Steinhoff D. Studies on cancer induction with colloidal silver and gold solutions in rats. Z Krebsforsch 1960;63:586-591 (German).
3. Furst A, Schlauder MC. Inactivity of two noble metals as carcinogens. J Environ Pathol Toxicol 1978;1(1):51-57.
4. Wijnhoven SW, Peijnenburg WJ, Herberts CA, Hagens WI, Oomen AG, Heugens EH, et al. Nano-silver–a review of available data and knowledge gaps in human and environmental risk assessment. Nanotoxicology 2009;3(2):109-138.
5. Maronpot RR. Chemical carcinogenesis. In: Haschek WM, Rousseaux CG, editors. Handbook of toxicologic pathology. San Diego: Academic Press; 1991, p. 91-129.
6. Barrett JC. Mechanisms of multistep carcinogenesis and carcinogen risk assessment. Environ Health Perspect 1993;100:9-20.
7. Combes RD. Detection of non-genotoxic carcinogens: major barriers to replacement of the rodent assay. In: van Zutphen LF, Balls M, editors. Proceedings of the 2nd World Congress on Alternatives and Animal Use in the Life Sciences; 1996 Oct 20-24; Utrecht, Netherlands. Amsterdam: Elsevier; 1997, p. 627-634.
8. Jiang X, Foldbjerg R, Miclaus T, Wang L, Singh R, Hayashi Y, et al. Multi-platform genotoxicity analysis of silver nanoparticles in the model cell line CHO-K1. Toxicol Lett 2013;222(1):55-63.
9. Li X, Xu L, Shao A, Wu G, Hanagata N. Cytotoxic and genotoxic effects of silver nanoparticles on primary Syrian hamster embryo (SHE) cells. J Nanosci Nanotechnol 2013;13(1):161-170.
10. Sahu SC, Njoroge J, Bryce SM, Yourick JJ, Sprando RL. Comparative genotoxicity of nanosilver in human liver HepG2 and colon Caco2 cells evaluated by a flow cytometric in vitro micronucleus assay. J Appl Toxicol 2014;34(11):1226-1234.
11. Castiglioni S, Caspani C, Cazzaniga A, Maier JA. Short- and long-term effects of silver nanoparticles on human microvascular endothelial cells. World J Biol Chem 2014;5(4):457-464.
12. Suliman Y AO, Ali D, Alarifi S, Harrath AH, Mansour L, Alwasel SH. Evaluation of cytotoxic, oxidative stress, proinflammatory and genotoxic effect of silver nanoparticles in human lung epithelial cells. Environ Toxicol 2015;30(2):149-160.
13. El Mahdy MM, Eldin TA, Aly HS, Mohammed FF, Shaalan MI. Evaluation of hepatotoxic and genotoxic potential of silver nanoparticles in albino rats. Exp Toxicol Pathol 2015;67(1):21-29.
14. Dobrzyńska MM, Gajowik A, Radzikowska J, Lankoff A, Dušinská M, Kruszewski M. Genotoxicity of silver and titanium dioxide nanoparticles in bone marrow cells of rats in vivo. Toxicology 2014;315:86-91.
15. Li Y, Bhalli JA, Ding W, Yan J, Pearce MG, Sadiq R, et al. Cytotoxicity and genotoxicity assessment of silver nanoparticles in mouse. Nanotoxicology 2014;8 Suppl 1:36-45.
16. Jung MH, Kim HR, Park YJ, Park DS, Chung KH, Oh SM. Genotoxic effects and oxidative stress induced by organic extracts of particulate matter (PM 10) collected from a subway tunnel in Seoul, Korea. Mutat Res 2012;749(1-2):39-47.
17. Sasaki K, Bohnenberger S, Hayashi K, Kunkelmann T, Muramatsu D, Poth A, et al. Photo catalogue for the classification of foci in the BALB/c 3T3 cell transformation assay. Mutat Res 2012;744(1):42-53.
18. Ponti J, Broggi F, Mariani V, De Marzi L, Colognato R, Marmorato

P, et al. Morphological transformation induced by multiwall carbon nanotubes on Balb/3T3 cell model as an in vitro end point of carcinogenic potential. Nanotoxicology 2013;7(2):221-233.
19. European Commission. Definition of a nanomaterial; 2011 [cited 2017 Oct 22]. Available from: http://ec.europa.eu/environment/chemicals/nanotech/faq/definition_en.htm.
20. Ng CT, Li JJ, Bay BH, Yung LY. Current studies into the genotoxic effects of nanomaterials. J Nucleic Acids 2010;2010:947859.
21. Kim HR, Kim MJ, Lee SY, Oh SM, Chung KH. Genotoxic effects of silver nanoparticles stimulated by oxidative stress in human normal bronchial epithelial (BEAS-2B) cells. Mutat Res 2011;726(2):129-135.
22. Kim HR, Park YJ, Shin DY, Oh SM, Chung KH. Appropriate in vitro methods for genotoxicity testing of silver nanoparticles. Environ Health Toxicol 2013;28:e2013003.
23. Li Y, Chen DH, Yan J, Chen Y, Mittelstaedt RA, Zhang Y, et al. Genotoxicity of silver nanoparticles evaluated using the Ames test and in vitro micronucleus assay. Mutat Res 2012;745(1-2):4-10.
24. Broggi F, Ponti J, Giudetti G, Franchini F, Stone V, García CP, et al. Silver nanoparticles induce cytotoxicity, but not cell transformation or genotoxicity on Balb3T3 mouse fibroblasts. BioNanoMaterials 2013;14(1-2):49-60.
25. Combes R, Balls M, Curren R, Fischbach M, Fusenig N, Kirkland D, et al. Cell transformation assays as predictors of human carcinogenicity. Altern Lab Anim 1999;27(5):745-767.
26. Tanaka N, Bohnenberger S, Kunkelmann T, Munaro B, Ponti J, Poth A, et al. Prevalidation study of the BALB/c 3T3 cell transformation assay for assessment of carcinogenic potential of chemicals. Mutat Res 2012;744(1):20-29.
27. Vanparys P, Corvi R, Aardema MJ, Gribaldo L, Hayashi M, Hoffmann S, et al. Application of in vitro cell transformation assays in regulatory toxicology for pharmaceuticals, chemicals, food products and cosmetics. Mutat Res 2012;744(1):111-116.
28. Ponti J, Sabbioni E, Munaro B, Broggi F, Marmorato P, Franchini F, et al. Genotoxicity and morphological transformation induced by cobalt nanoparticles and cobalt chloride: an in vitro study in Balb/3T3 mouse fibroblasts. Mutagenesis 2009;24(5):439-445.
29. Choo WH, Park CH, Jung SE, Moon B, Ahn H, Ryu JS, et al. Long-term exposures to low doses of silver nanoparticles enhanced in vitro malignant cell transformation in non-tumorigenic BEAS-2B cells. Toxicol In Vitro 2016;37:41-49.